

Original article

Stasis imaging predicts the risk of cardioembolic events related to acute myocardial infarction: the ISBITAMI study



Elena Rodríguez-González,^{a,b,c} Pablo Martínez-Legazpi,^{c,d,*} Teresa Mombiela,^{a,b,c}
 Ana González-Mansilla,^{a,b,c} Antonia Delgado-Montero,^{a,b,c} Juan A. Guzmán-De-Villoria,^{e,f}
 Fernando Díaz-Otero,^g Raquel Prieto-Arévalo,^{a,b,c} Miriam Juárez,^{a,b,c} María del Carmen García del Rey,^{a,b,c}
 Pilar Fernández-García,^{e,f} Óscar Flores,^h Andrea Postigo,^{a,b,c} Raquel Yotti,^{a,b,c} Manuel García-Villalba,ⁱ
 Francisco Fernández-Avilés,^{a,b,c} Juan C. del Álamo,^j and Javier Bermejo^{a,b,c}

^a Servicio de Cardiología, Hospital General Universitario Gregorio Marañón, Instituto de Investigación Sanitaria Gregorio Marañón, Madrid, Spain

^b Facultad de Medicina, Universidad Complutense de Madrid, Madrid, Spain

^c Centro de Investigación Biomédica en Red Enfermedades Cardiovasculares (CIBERCV), Spain

^d Departamento de Física Matemática y Fluidos, Facultad de Ciencias, Universidad Nacional de Educación a Distancia (UNED), Madrid, Spain

^e Servicio de Radiología, Hospital General Universitario Gregorio Marañón, Instituto de Investigación Sanitaria Gregorio Marañón, Madrid, Spain

^f Centro de Investigación Biomédica en Red de Salud Mental (CIBERSAM), Madrid, Spain

^g Servicio de Neurología, Hospital General Universitario Gregorio Marañón, Instituto de Investigación Sanitaria Gregorio Marañón, Madrid, Spain

^h Departamento de Ingeniería Aeroespacial, Universidad Carlos III de Madrid, Leganés, Madrid, Spain

ⁱ TU Wien, Institute of Fluid Mechanics and Heat Transfer, Vienna, Austria

^j Mechanical Engineering Department, Center for Cardiovascular Biology, Institute for Stem Cell and Regenerative Medicine, University of Washington, Seattle, United States

Article history:

Received 5 January 2024

Accepted 25 April 2024

Available online 8 May 2024

Keywords:

Ischemic stroke

ST-segment elevation myocardial infarction

Echocardiography

Blood stasis

Cardioembolism

ABSTRACT

Introduction and objectives: In the setting of ST-segment elevation myocardial infarction (STEMI), imaging-based biomarkers could be useful for guiding oral anticoagulation to prevent cardioembolism. Our objective was to test the efficacy of intraventricular blood stasis imaging for predicting a composite primary endpoint of cardioembolic risk during the first 6 months after STEMI.

Methods: We designed a prospective clinical study, Imaging Silent Brain Infarct in Acute Myocardial Infarction (ISBITAMI), including patients with a first STEMI, an ejection fraction $\leq 45\%$ and without atrial fibrillation to assess the performance of stasis metrics to predict cardioembolism. Patients underwent ultrasound-based stasis imaging at enrollment followed by heart and brain magnetic resonance at 1-week and 6-month visits. From the stasis maps, we calculated the average residence time, R_T , of blood inside the left ventricle and assessed its performance to predict the primary endpoint. The longitudinal strain of the 4 apical segments was quantified by speckle tracking.

Results: A total of 66 patients were assigned to the primary endpoint. Of them, 17 patients had 1 or more events: 3 strokes, 5 silent brain infarctions, and 13 mural thromboses. No systemic embolisms were observed. R_T (OR, 3.73; 95%CI, 1.75-7.9; $P < .001$) and apical strain (OR, 1.47; 95%CI, 1.13-1.92; $P = .004$) showed complementary prognostic value. The bivariate model showed a c-index = 0.86 (95%CI, 0.73-0.95), a negative predictive value of 1.00 (95%CI, 0.94-1.00), and positive predictive value of 0.45 (95%CI, 0.37-0.77). The results were confirmed in a multiple imputation sensitivity analysis. Conventional ultrasound-based metrics were of limited predictive value.

Conclusions: In patients with STEMI and left ventricular systolic dysfunction in sinus rhythm, the risk of cardioembolism may be assessed by echocardiography by combining stasis and strain imaging. Registered at ClinicalTrials.gov (NCT02917213).

© 2024 Sociedad Española de Cardiología. Published by Elsevier España, S.L.U. This is an open access article under the CC BY-NC-ND license (<http://creativecommons.org/licenses/by-nc-nd/4.0/>).

La imagen de estasis predice el riesgo de eventos cardioembólicos tras el infarto agudo de miocardio: el estudio ISBITAMI

RESUMEN

Introducción y objetivos: Tras el infarto agudo de miocardio con elevación del segmento ST (IAMCEST), los biomarcadores por imagen pueden ser útiles para guiar la anticoagulación oral en la prevención primaria de la cardioembolia. Nuestro objetivo es probar la eficacia de la imagen de estasis intraventricular como predictora del riesgo cardioembólico después de un IAMCEST.

Palabras clave:

Accidente cerebrovascular

Infarto de miocardio con elevación del

segmento ST

Ecocardiografía

SEE RELATED CONTENT:

<https://doi.org/10.1016/j.rec.2024.06.009>

* Corresponding author.

E-mail address: legazpi.pablo@ccia.uned.es (P. Martínez-Legazpi).

<https://doi.org/10.1016/j.rec.2024.04.007>

1885-5857/© 2024 Sociedad Española de Cardiología. Published by Elsevier España, S.L.U. This is an open access article under the CC BY-NC-ND license (<http://creativecommons.org/licenses/by-nc-nd/4.0/>).

Métodos: Se diseñó un estudio clínico prospectivo, *Imaging Silent Brain Infarct in Acute Myocardial Infarction* (ISBITAMI), que incluyó a pacientes con un primer IAMCEST y fracción de eyección del ventrículo izquierdo $\leq 45\%$, sin fibrilación auricular, para evaluar el desempeño de las métricas de estasis en la predicción de la cardioembolia. En la inclusión, se obtuvieron imágenes de estasis por ultrasonido, seguidas de resonancia magnética cardíaca y cerebral en 2 visitas tras 1 semana y 6 meses. Usando los mapas de estasis, calculamos el tiempo de residencia promedio, R_T , de la sangre dentro del VI y evaluamos su eficacia para predecir el objetivo primario. El *strain* apical longitudinal en los 4 segmentos apicales se cuantificó mediante *speckle tracking*.

Resultados: Un total de 66 pacientes completaron el periodo de seguimiento. De ellos, 17 pacientes sufrieron 1 o más eventos: 3 ictus, 5 infartos cerebrales silentes y 13 trombosis murales. No se observaron embolias sistémicas. El R_T (OR = 3,73; IC95%, 1,75-7,97; $p < 0,001$) y el *strain* apical (OR = 1,47; IC95%, 1,13-1,92; $p = 0,004$) mostraron un valor pronóstico complementario. El modelo bivariado mostró un índice $c = 0,86$ (IC95%, 0,73-0,95), un valor predictivo negativo de 1,00 (IC95%, 0,94-1,0) y un valor predictivo positivo de 0,45 (IC95%, 0,37-0,77). Las métricas convencionales tuvieron un valor predictivo limitado.

Conclusiones: En pacientes con IAMCEST y disfunción sistólica del VI en ritmo sinusal, el riesgo de cardioembolia puede estimarse usando ecocardiografía y combinando imágenes de estasis y deformación. Registrado en ClinicalTrials.gov (NCT02917213).

© 2024 Sociedad Española de Cardiología. Publicado por Elsevier España, S.L.U. Este es un artículo Open Access bajo la CC BY-NC-ND licencia (<http://creativecommons.org/licencias/by-nc-nd/4.0/>).

Abbreviations

CMR: cardiac magnetic resonance
LVT: left ventricular thrombus
OAC: oral anticoagulation
 R_T : blood residence time
SBI: silent brain infarction
STEMI: ST-segment elevation myocardial infarction

INTRODUCTION

In the month following an ST-segment elevation myocardial infarction (STEMI), the adjusted risk for ischemic stroke is 30 times higher than in the general population.¹ Oral anticoagulation (OAC) is highly effective in preventing prevent stroke, but its benefits are neutralized by the increased bleeding risk.^{2–4} Therefore, to prevent cardioembolism in the first few weeks after STEMI, a personalized risk assessment would help to select candidates for OAC.

In addition to atrial fibrillation (AF), 2 major risk factors for cardioembolism in the setting of STEMI are blood stagnation inside the left ventricle (LV) and endocardial damage.^{5,6} The latter is closely related to abnormal regional function of the ischemic territories and can therefore be adequately addressed by strain imaging. Concerning the former, a method to visualize and quantify blood stasis inside the heart from conventional echocardiographic data has recently been implemented.^{7,8} Using this method, a global biomarker to account for the cardioembolic risk related to blood stasis has been proposed: the *residence time* (R_T) of blood in the LV. This metric can be interpreted as the number of cycles blood spends during its transit through the LV.^{8,9} Spatiotemporal maps of the R_T are a valuable tool for assessing the regions prone to blood stagnation, and preliminary proof-of-concept animal and clinical studies have shown the potential of R_T to account for the risk of STEMI-related mural thrombosis and cerebral microembolisms.^{10,11}

This study is the first clinical trial designed to prospectively assess the efficacy of stasis imaging to predict brain and heart cardioembolic events during the 6 months following STEMI. A composite primary endpoint integrated neurological events and subclinical outcomes from heart and brain imaging examinations.

METHODS

Overall design

The Imaging Silent Brain Infarct in Acute Myocardial Infarction (ISBITAMI) prospective clinical study was first registered in 2016 (registration number NCT02917213). We screened all patients admitted to our institution with the following inclusion criteria: a first STEMI with or without undergoing revascularization and an LV ejection fraction (EF) $\leq 45\%$ at admission, age ≥ 18 years, the presence of sinus rhythm, and no history of AF. Exclusion criteria consisted of any medical history of stroke or transient ischemic attack, ongoing OAC therapy, or a formal indication for this therapy, any contraindication for magnetic resonance examination, a history of cardiogenic shock, a history of recovered sudden death, or any other potential cause of acute brain damage due to hypoperfusion, a primary valve disease $\geq 3+$ severity, a diagnosis of carotid artery disease with $> 50\%$ stenosis, a history of prothrombotic disease, and reluctance to sign the written informed consent. Any history of AF (either clinically or subclinically detected in 24-hour Holter tests or any cardiac monitoring device) was also an exclusion criterion. The study was approved by the Ethics Committee of *Hospital Gregorio Marañón*, and all patients provided written informed consent. The study was academically funded, and the *Fundación para la Investigación Biomédica Hospital Gregorio Marañón* was the sole sponsor. The work conforms to the principles outlined in the Declaration of Helsinki.

Study endpoint

The primary composite endpoint integrated the incidence of any of the following events between the inclusion and the 6-month follow-up visits: a) a stroke or transient ischemic attack, b) a clinically apparent peripheral systemic embolism in any arterial territory, c) an acute or subacute silent brain infarct (SBI) lesion dated after symptom onset, assessed by brain magnetic resonance, or d) a diagnosis of LV mural thrombosis (LVT), either by contrast-echocardiography or late-gadolinium enhanced cardiac magnetic resonance (CMR) studies. Patients with any endpoint-positive event were followed up to ensure resolution with usual care. Stroke was clinically assessed, and additional imaging tests (eg, brain computed tomography) were carried out when necessary.

Conventional cardiac and brain imaging

All patients underwent 4 imaging examinations: at screening (assessment of inclusion criteria by echocardiography), within 24 to 72 hours after admission (enrollment study, echocardiography, and stasis imaging), at 1 week (echocardiography and brain and heart magnetic resonance), and 6 months after enrollment (echocardiography and brain and heart magnetic resonance, see methods of the supplementary data for details).

Ancillary variables

Clinical and outcome data were collected at the enrollment and 6-month visits. These included all clinical events, ongoing medications, hematological and biochemical assessments, Beck Depression Inventory, and the Mini-Mental State Examinations. We performed transcranial Doppler and carotid duplex ultrasound examinations in patients with a primary endpoint to rule out alternative extracardiac causes of embolisms. Implantable cardiac loop monitoring devices (iLINO, Medtronic, Ireland) were placed in a random sample of 31 patients to exclude asymptomatic AF during the 6-month follow-up. Additional screening for AF using conventional 24-hour Holter monitoring was scheduled if patients reported palpitations, syncope, or any other symptoms potentially caused by AF.

Intraventricular stasis imaging

From the echocardiograms performed at enrollment, we calculated 2-dimensional, time-resolved (2D+t) blood flow fields inside the LV using color-Doppler velocimetry.¹² Blood velocity data were used to integrate a forced advection equation with the purpose of mapping and quantifying the residence time, R_T , an index that accounts for the number of cardiac cycles a volume of blood spends inside the LV.⁷ At the end of the 8th beat, the estimated period taken for a full washout in a normal LV,⁹ we collected the average R_T inside the LV as a single metric of stasis. The full process is summarized in figure 1. All image processing was performed blind to endpoint adjudication. The reproducibility of stasis indices has been reported elsewhere.⁹ Full methodological details can be found in the methods of the supplementary data.

Statistical analysis

The sample size of the study was established at $n = 92$ patients to achieve an 85% power to reach significance ($P < .05$) with a c -index > 0.75 , assuming a 15% incidence of the primary endpoint and a 15% attrition rate. Data are described as median [interquartile range] unless otherwise indicated. We used the Wilcoxon rank-sum and Fisher exact tests to compare quantitative variables and proportions, respectively. Odds ratios (OR) and their 95% confidence intervals (95%CI) are reported for these models. The interplay between clinical predictors, R_T , and the primary endpoint was further investigated using Pearson correlation analyses. We used receiver operating characteristic (ROC) analyses to estimate the c -index, its 95%CI, and its statistical significance. Cutoffs were selected by using the Youden method, weighted to penalize for false negatives. The medians (and 95%CI) of performance metrics of these cutoffs (sensitivity, specificity, positive and negative predictive values) were calculated by bootstrap of 2000 replicates.

The analyses are reported for patients who reached the end of the follow-up protocol or could be allocated to the primary endpoint because they had an event before that time (figure 2). To account for losses to follow-up, we performed a sensitivity analysis

to avoid verification bias (see methods of the supplementary data). Statistical analyses were performed in R (v. 4.1.3) and P values $< .05$ were considered significant.

RESULTS

Study population

Patient recruitment started in January 2017, and the last patient follow-up ended in January 2022. From an initial group of 92 screened patients, a total of 66 patients were assigned to the primary endpoint: 63 patients completed the 6-month follow-up and there were 3 patients without follow-up but who experienced a positive endpoint at the 1-week visit (figure 2). Four patients died after enrollment, precluding adjudication of the primary endpoint: 1 due to arrhythmic storm, 1 due to acute stent thrombosis, and 2 due to an unknown cause at home.

The median [IQR] age was 58 [51-67] years, and 22% of the patients were women (table 1). Sixty-two patients underwent primary percutaneous coronary intervention, and the STEMI location was anterior in 59 patients. Four patients did not undergo primary PCI either because they underwent a PCI following thrombolysis ($n = 2$) or because a conservative strategy was chosen due to advanced age ($n = 1$) or PCI was contraindicated by unsuitable anatomy ($n = 1$). EF on echocardiography at enrollment was 41% [36% to 48%], and values obtained by CMR at 1 week were similar (tables 2 and table 3).

Cardioembolic events

Twenty-one events were recorded in 17 of the 66 studied patients (25%). Three patients had an ischemic stroke. Of them, 1 occurred after the diagnosis of LVT despite prior initiation of oral anticoagulants. Another stroke occurred 1 week after detection of an SBI. Twelve patients showed LVT, 2 of them showing accompanying SBIs at the same 1-week visit. Finally, 2 patients were diagnosed with SBIs without additional events (1 at the 1-week visit and the other at the 6-month visit). No peripheral systemic embolisms were clinically identified (table 4).

Carotid duplex and transcranial Doppler ruled out alternative etiologies of the neurological events in all patients with SBI or stroke. No AF was identified during the 6-month period in the 31 randomly selected patients who received an implantable cardiac rhythm monitoring device. There were no differences in clinical, hematological, or biochemical variables among patients with and without the primary endpoint. There were no differences in the Beck Depression Inventory or Mini-Mental State Examinations among patients with and without the primary endpoint, either at enrollment or at the 6-month follow-up visit. Myocardial infarction was in an anterior location in all patients with a primary endpoint.

Imaging predictors of the primary endpoint

Patients with a primary endpoint showed a larger myocardial infarct size on CMR than those without an endpoint (37% [29% to 37%] vs 21% [15% to 31%] of total myocardial mass, respectively, $P = .06$). Enrollment echocardiographic examinations showed lower EF values in patients with a primary endpoint (38% [34%-42%]) than in those without (42% [36% to 51%]; $P = .02$). In addition, apical strain was higher in patients with a primary endpoint than in those free of events: -4.8% [-7.4% , -3.6%] vs -7.8% [-9.7% , -6.3%] ($P < .001$).

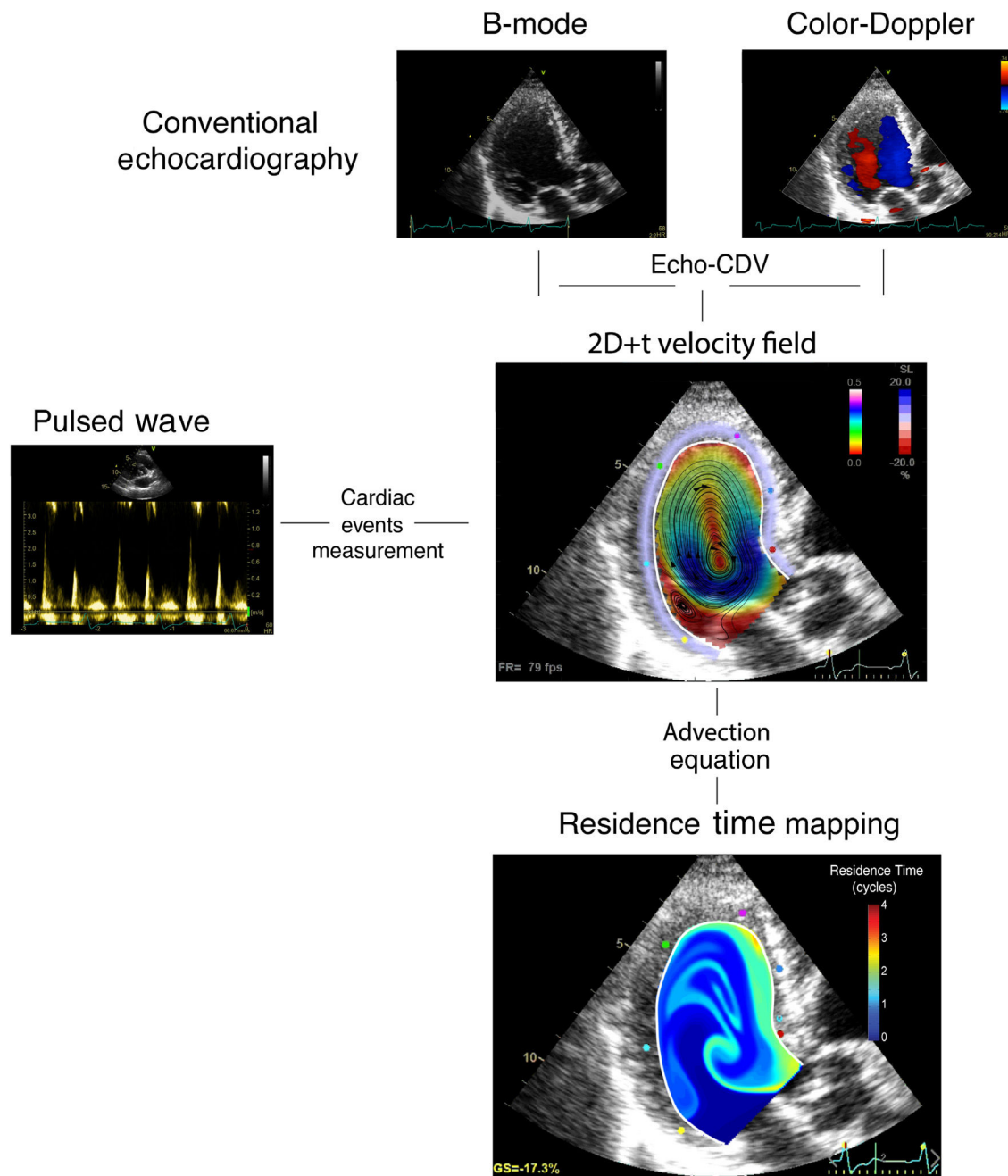


Figure 1. Stasis mapping workflow. Echo-CDV, echocardiography Color-Doppler velocimetry; 2D+t, 2-dimensional time-resolved.

The c-indices of EF, calculated by echocardiography and CMR, to predict the primary endpoint were 0.69 (95%CI, 0.55-0.82) and 0.55 (95%CI, 0.40-0.69), respectively. However, the predictive power of EF on ultrasound was related to the fact that EF was $\leq 50\%$ in all patients with a primary endpoint; the primary endpoint was not identified in any patient whose EF reached 50% from inclusion to enrollment. Among patients who persisted with an EF $\leq 50\%$, the c-index of EF was 0.55 (95%CI, 0.38-0.72; $P = .6$). Of the CMR indices, only myocardial infarct size showed moderate performance, but without significance, c-index 0.67 (95%CI, 0.49-0.84; $P = .1$).

The c-index of apical strain to predict the primary endpoint was 0.75 (0.62-0.88) with an odds-ratio of 1.48 (95%CI, 1.13-1.92; $P = .002$, [table 1 of the supplementary data](#)) per unit. The c-index of

R_T was 0.82 (95%CI, 0.71-0.92) with an OR of 3.73 (95%CI, 1.75-7.96) per cycle ($P < .001$, [table 1 of the supplementary data](#) and [figure 3](#)). In a multivariate model including EF, R_T and apical strain to predict the primary endpoint, only the latter 2 showed statistical significance (P values = .80; $P < .001$ and $P = .03$, respectively, $R^2 = 0.3$).

Predictive accuracy was highest in the bivariate model including R_T and apical strain: c-index = 0.86 (0.73-0.95), with both apical strain (OR, 1.41; 95%CI, 1.05-1.90) and R_T (OR, 3.48; 95%CI, 1.49-8.13) retaining significant predictive value ($P = .02$ and $.003$, respectively, [figure 3](#)). In the bivariate model, sensitivity, specificity, and positive and negative predictive values were 1.00 (95%CI, 0.88-1.00), 0.54 (95%CI, 0.37-0.91), 0.45 (95%CI, 0.37-0.77), and 1.00 (95%CI, 0.94-1.00), respec-

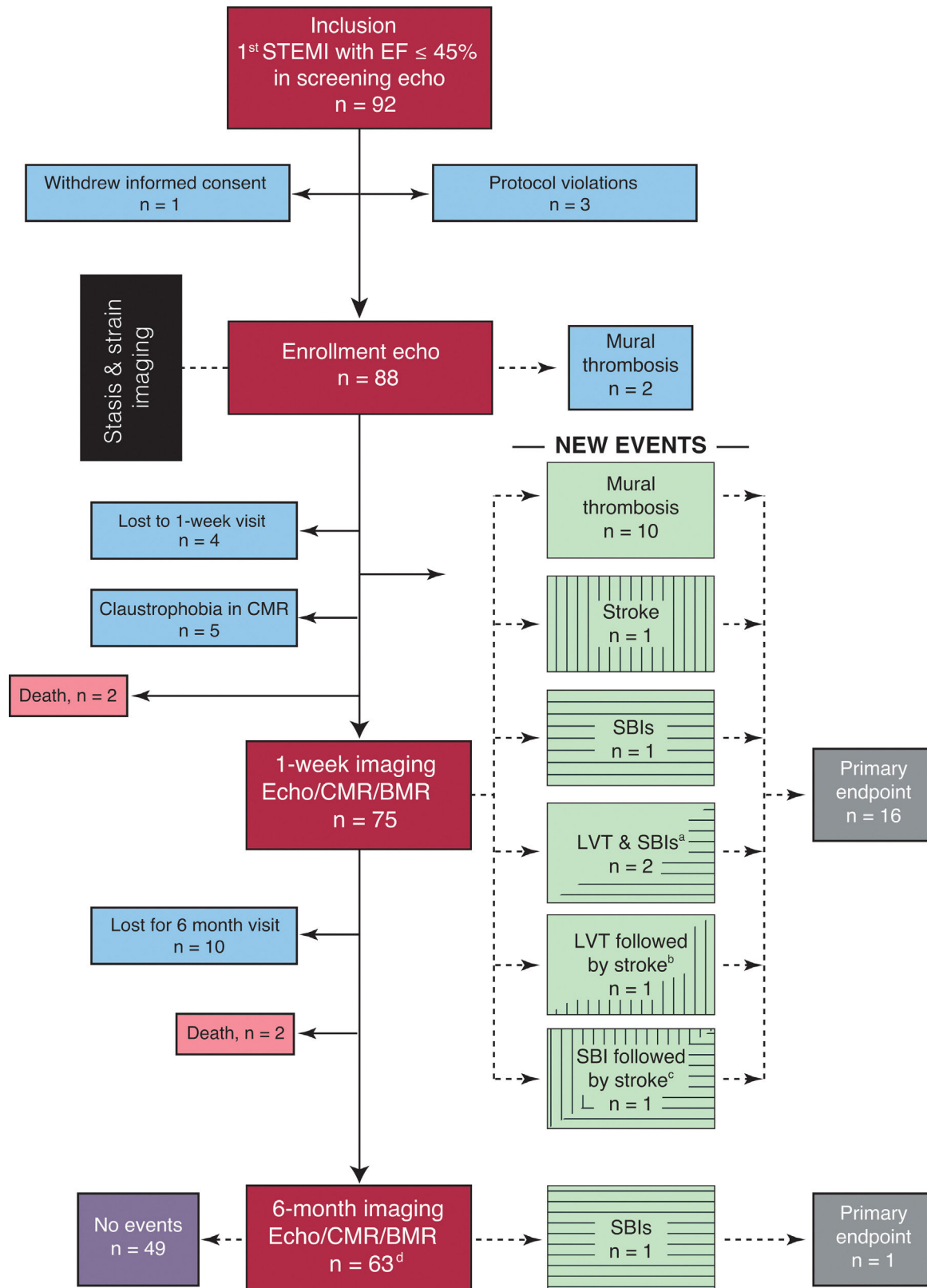


Figure 2. Flow diagram of the ISBITAMI study and the primary endpoints. BMR, brain magnetic resonance; CMR, cardiac magnetic resonance; Echo, echocardiography; EF, ejection fraction; LVT, left ventricular mural thrombosis; STEMI, ST-segment elevation myocardial infarction.

^a Two patients simultaneously showed SBIs and LVT.

^b One patient had a stroke 4 days after LVT was imaged despite being under OAC therapy.

^c One patient had a stroke 1 week after an SBI was imaged.

^d Twelve patients were lost to follow-up. Of them, 3 patients had already experienced the endpoint, recorded at the 1-week visit.

Table 1
Clinical data

	All patients	Negative PE	Positive PE	P
No.	66	49	17	
Age, y	58 [51-67]	59 [52-66]	57 [47-72]	.9
Male sex	52 (78)	37 (75)	15 (88)	.7
Body mass index, kg/m²	27.4 [25.4-29.0]	27.4 [25.6-28.8]	27.3 [25.0-29.7]	.9
Body surface area, m²	1.91 [1.78-2.05]	1.89 [1.77-2.05]	1.94 [1.86-2.05]	.2
Systolic blood pressure, mmHg	120 [105-130]	120 [106-130]	112 [105-120]	.4
Diastolic blood pressure, mmHg	71 [60-80]	72 [60-80]	70 [60-80]	.8
Heart rate, bpm	69 [65-69]	70 [65-79]	69 [65-79]	.9
Clinical data				
<i>Diabetes mellitus</i>	10 (15)	9 (18)	1 (5.9)	.3
<i>Dyslipidemia</i>	28 (44)	22 (45)	6 (35)	.4
<i>Hypertension</i>	27 (43)	20 (41)	7 (41)	.9
<i>Smoker</i>	30 (51)	23 (47)	7 (41)	.5
<i>Primary coronary intervention</i>	62 (94)	45 (92)	17 (100)	.9
<i>Time to reperfusion, min</i>	240 [145-383]	240 [145-383]	218 [170-375]	>.9
<i>Anterior AMI location</i>	59 (90)	42 (85)	17 (100)	.2
<i>Killip-Kimball class</i>				.8
I	56 (84)	42 (86)	14 (82)	
II	7 (11)	5 (11)	2 (12)	
III	2 (3)	1 (2.2)	1 (5.9)	
Drug therapy at discharge Chronic				
<i>Beta-blockers</i>	57 (86)	41 (83)	16 (94)	>.9
<i>ACEI/ARBs</i>	57 (86)	41 (83)	16 (94)	>.9
<i>Aspirin</i>	65 (98)	49 (100)	16 (94)	.3
<i>Clopidogrel</i>	15 (22)	3 (7.0)	12 (69)	<.001
<i>Ticagrelor</i>	28 (42)	26 (53)	2 (13)	.005
<i>Prasugrel</i>	20 (30)	18 (37)	2 (13)	.11
Laboratory				
<i>Hemoglobin, g/dL</i>	15.1 [14.7-15.9]	15.1 [14.7-15.9]	15.1 [14.8-16.0]	>.9
<i>Platelet count × 10⁹/L</i>	225 [205-266]	233 [212-268]	207 [187-229]	.07
<i>Creatinine, mg/dL</i>	0.92 [0.78-0.98]	0.91 [0.76-0.97]	0.95 [0.83-1.04]	.3
<i>Peak high sensitivity troponin, ng/mL</i>	25 260 [5751-50 000]	14 777 [5133-50 000]	39 359 [737- 50 000]	.2
<i>Creatine kinase, IU/L</i>	1996 [936-2842]	1735 [932-2919]	2034 [1760-2409]	.7
<i>NT-proBNP, pg/mL</i>	1210 [155-2270]	1210 [155-2392]	1178 [421-1854]	.8
Neuro-psychiatric evaluation				
<i>Beck Depression Inventory</i>				
<i>Enrollment</i>	0.0 [0.0-3.5]	0.0 [0.0-4.8]	0.0 [0.0-2.0]	.8
<i>6-mo</i>	2.0 [0.0-6.0]	2.0 [0.0-7.0]	2.0 [0.0-5.0]	.9
Δ				
<i>Mini-Mental State Examination</i>				
<i>Enrollment</i>	30.00 [28.00-30.00]	30.0 [28.7-30.00]	30.0 [27.0-30.0]	.9
<i>6-mo</i>	30.00 [27.75-30.00]	30.0 [27.7-31.00]	30.0 [26.7-30.0]	.7
Δ				

ACEI, angiotensin converting enzyme inhibitors; ARB, angiotensin receptor blockers; AMI, acute myocardial infarction; mo, month; NT-proBNP, N-terminal pro-B-type natriuretic peptide; PE, primary endpoint.

Values are expressed as the median [interquartile range] unless otherwise indicated.

tively. The c-index of the bivariate model was 0.81 (95%CI, 0.68-0.84) among patients with an EF ≤ 50%. The final model for the risk of the primary endpoint was $\log(\text{risk}) = -2.9 + 0.34 \cdot \text{strain} (\%) + 1.24 \cdot R_T (\text{cycles})$. The sensitivity analysis confirmed similar performance of apical strain and R_T to predict the primary endpoint in the imputed set (table 1 of the supplementary data). Figure 4 and videos 1 and 2 of the supplementary data show illustrative examples from patients with and without the primary endpoint. Video 3 of the

supplementary data shows the R_T map in a healthy volunteer for comparison.

DISCUSSION

This proof-of-concept study suggests a potential value of combining strain imaging and stasis biomarkers to account for cardioembolic risk after STEMI. By exploiting the well-known

Table 2
Ultrasound imaging at enrollment

No.	All patients 66	Negative PE 49	Positive PE 17	P
<i>Echocardiography</i>				
LV end-diastolic volume index, mL/m ²	49 [43-58]	51 [43-58]	49 [46-58]	.8
LV end-systolic volume index, mL/m ²	29 [23-36]	28 [21-35]	30 [26-38]	.3
Stroke volume index (B-mode), mL/m ²	20 [18-24]	21 [18-25]	18 [16-21]	.08
Stroke volume index (Doppler), mL/m ²	26 [21-28]	26 [22-28]	25 [21-28]	.6
LV ejection fraction, %	41 [36-48]	42 [36-51]	38 [34-42]	.02
Sphericity ratio	0.53 [0.48-0.57]	0.54 [0.49-0.57]	0.53 [0.47-0.58]	.6
E-wave velocity, cm/s	54 [45-65]	54 [46-70]	52 [44-59]	.4
A wave velocity, cm/s	70 [55-78]	70 [63-81]	61 [45-75]	.06
E/A wave ratio	0.77 [0.63-1.03]	0.77 [0.62-1.00]	0.76 [0.63-1.20]	.6
E/e'	8.9 [7.2-10.8]	9.1 [7.5-10.9]	7.9 [7.0-10.5]	.2
E-wave penetration index	0.95 [0.70-1.12]	0.95 [0.73-1.13]	0.88 [0.57-1.08]	.4
Global peak systolic longitudinal strain, %	−9.1 [−10.7 to −8.1]	−9.6 [−11.3 to −8.5]	−7.93 [−9.1 to −7.3]	.008
Apical peak systolic longitudinal strain, %	−7.4 [−9.0 to −4.8]	−7.8 [−9.7 to −6.3]	−4.8 [−7.4 to −3.6]	.001
Wall motion score index	2.0 [1.8-2.1]	2.0 [1.8-2.1]	2.00 [1.9-2.2]	.2
<i>Stasis imaging</i>				
Intraventricular blood residence time, cycles	2.94 [2.54-3.61]	2.80 [2.45-3.26]	3.59 [3.19-5.11]	<.001

LV, left ventricle; PE, primary endpoint.

Values are expressed as the median [interquartile range] unless otherwise indicated.

Table 3
Cardiac imaging at the 1-week and 6-month visits

	1-Week visit			6-Month visit		
	Negative PE	Positive PE	P	Negative PE	Positive PE	P
<i>Echocardiography</i>						
LV end-diastolic volume index, mL/m ²	50 [43-60]	54 [47-60]	.4	52 [45-61]	66 [55-73]	.07
LV end-systolic volume index, mL/m ²	28 [21-32]	32 [29-38]	.076	26 [21-33]	33 [28-43]	.04
Stroke volume index (B-mode), mL/m ²	23 [19-26]	22 [20-23]	.3	27 [24-29]	30 [20-41]	.4
Stroke volume index (Doppler), mL/m ²	26 [22-31]	30 [27-33]	.2	31 [26-38]	30 [27-38]	.8
LV ejection fraction, %	46 [40-53]	39 [37-42]	.008	53 [45-57]	47 [41-50]	.2
Sphericity ratio	0.54 [0.50-0.57]	0.54 [0.49-0.56]	.6	0.56 [0.51-0.61]	0.57 [0.48-0.58]	.5
E-wave velocity, cm/s	61 [50-72]	59 [43-70]	.3	62 [48-78]	57 [45-60]	.2
A wave velocity, cm/s	68 [58-78]	61 [40-71]	.1	66 [52-80]	58 [48-70]	.08
E/A wave ratio	0.81 [0.74-1.28]	1.02 [0.66-1.62]	.6	0.92 [0.68-1.48]	1.00 [0.93-1.44]	.5
E/e'	9.5 [8.1-12.2]	8.8 [7.5-10.2]	.2	8.3 [7.1-9.8]	8.5 [6.8-10.7]	.9
E-wave penetration index	1.12 [0.86-1.31]	0.79 [0.71-1.28]	.2	1.35 [0.99-1.63]	1.06 [0.80-1.34]	.2
<i>CMR</i>						
LV end-diastolic volume index, mL/m ²	87 [82-98]	98 [84-106]	.2	91 [76-100]	99 [92-109]	.1
LV end-systolic volume index, mL/m ²	50 [44-57]	59 [48-62]	.2	44 [37-58]	53 [44-64]	.2
Stroke volume index, mL/m ²	38.1 [32.0-42.3]	39.7 [35.7-44.5]	.1	42 [39-50]	45 [41-49]	.4
LV ejection fraction, %	41 [38-48]	41 [39-44]	.6	49 [42-55]	48 [43-51]	.2
LV mass index, g/m ²	58 [53-62]	64 [57-68]	.09	49 [43-55]	54 [48-58]	.2
Infarct size, g	24 [19-33]	37 [26-42]	.2	20 [12-26]	17 [14-36]	.8
Infarct size, %	21 [15-31]	32 [29-38]	.06	21 [14-25]	15 [12-30]	.9

CMR, cardiac magnetic resonance; LV, left ventricle; PE, primary endpoint.

Values are expressed as the median [interquartile range] unless otherwise indicated.

mechanistic associations between stasis, local damage, and thrombosis, we implemented an ultrasound-based model that performed better than traditional indices, such as EF, to predict cardioembolic events. The prediction efficacy suggests a potential for grading the risk of cardioembolism based on strain and stasis imaging (figure 5).

To our knowledge, this is the first study to prospectively address SBIs in the setting of STEMI. SBIs refer to those lesions in the brain parenchyma that meet the imaging characteristics of an infarct, but which are not associated with clinical signs or symptoms of stroke or transient ischemic attack. SBIs are frequently identified in patients with systolic dysfunction,¹³ a

Table 4
Composite endpoint

	No. (%)	Comments
Total patients	66	
Patients who reached composite endpoint	17 (26)	
At 1-wk visit (n=66)	16 (24)	3 strokes (1 coexisting with an SBI and 1 coexisting with LVT). 12 LVT (2 coexisting with SBIs); 1 SBI.
At 6-mo visit (n=63)	1 (1)	1 SBI.
Left ventricular mural thrombosis		
At 1-wk CMR (n=66)	13 (19)	11 disappeared after 6 mo OAC and were not present at 6-mo CMR. One was followed by a stroke 4 d after the visit despite OAC.
At 6-mo CMR (n=63)	0 (0)	2 still present from 1-wk CMR.
Silent brain infarct		
At 1-wk brain MR (n=66)	4 (6)	2 coexisting with LVT at 1-wk CMR.
At 6-mo brain MR (n=63)	1 (2)	1 not present at 1-wk BMR and without LVT.
Stroke		
Total (n=66)	3 (4)	First: 4-d after LVT at 1-wk CMR and under OAC; second: 1 wk after SBI found at 1-wk BMR; third: without LVT or SBI at the 1-wk MRI.
Peripheral embolism (other territories)		
At enrollment (n=66)	0 (0)	
At 6-mo follow-up (n=63)	0 (0)	

BMR, brain magnetic resonance; CMR, cardiac magnetic resonance; MR, magnetic resonance; MRI, magnetic resonance imaging; LV, left ventricle; LVT, left ventricle mural thrombosis; mo, month; OAC, oral anticoagulation; SBI, silent brain infarct; wk, week.

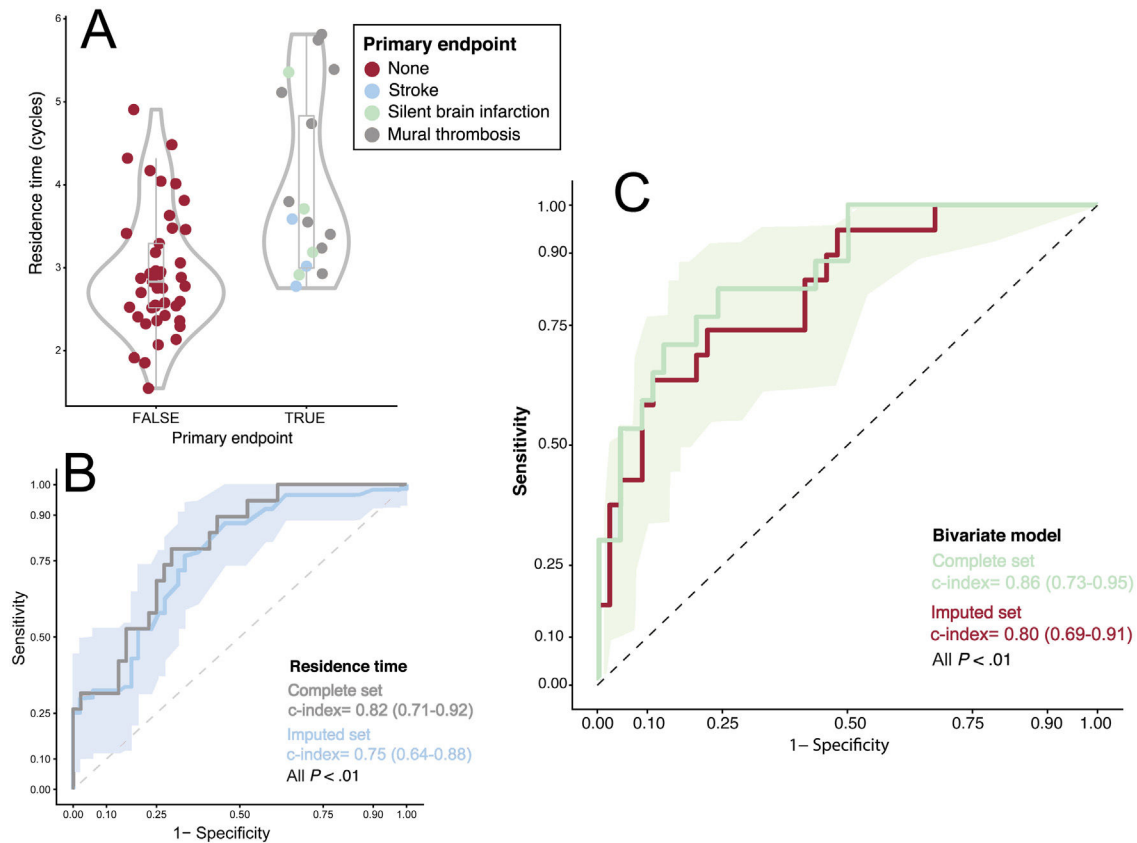


Figure 3. Relationship between residence time and the primary endpoint. A, violin and boxplots; the primary endpoint is colored upon its etiology. B, ROC curve for the performance of R_T for predicting the primary endpoint (complete and imputed sets). C, ROC curve for the performance of the bivariate model (R_T + apical strain) for predicting the primary endpoint (complete and imputed sets). The ribbons on panels B and C show the sensitivity and 95% confidence interval of the ROC curve calculated for the imputed set. ROC

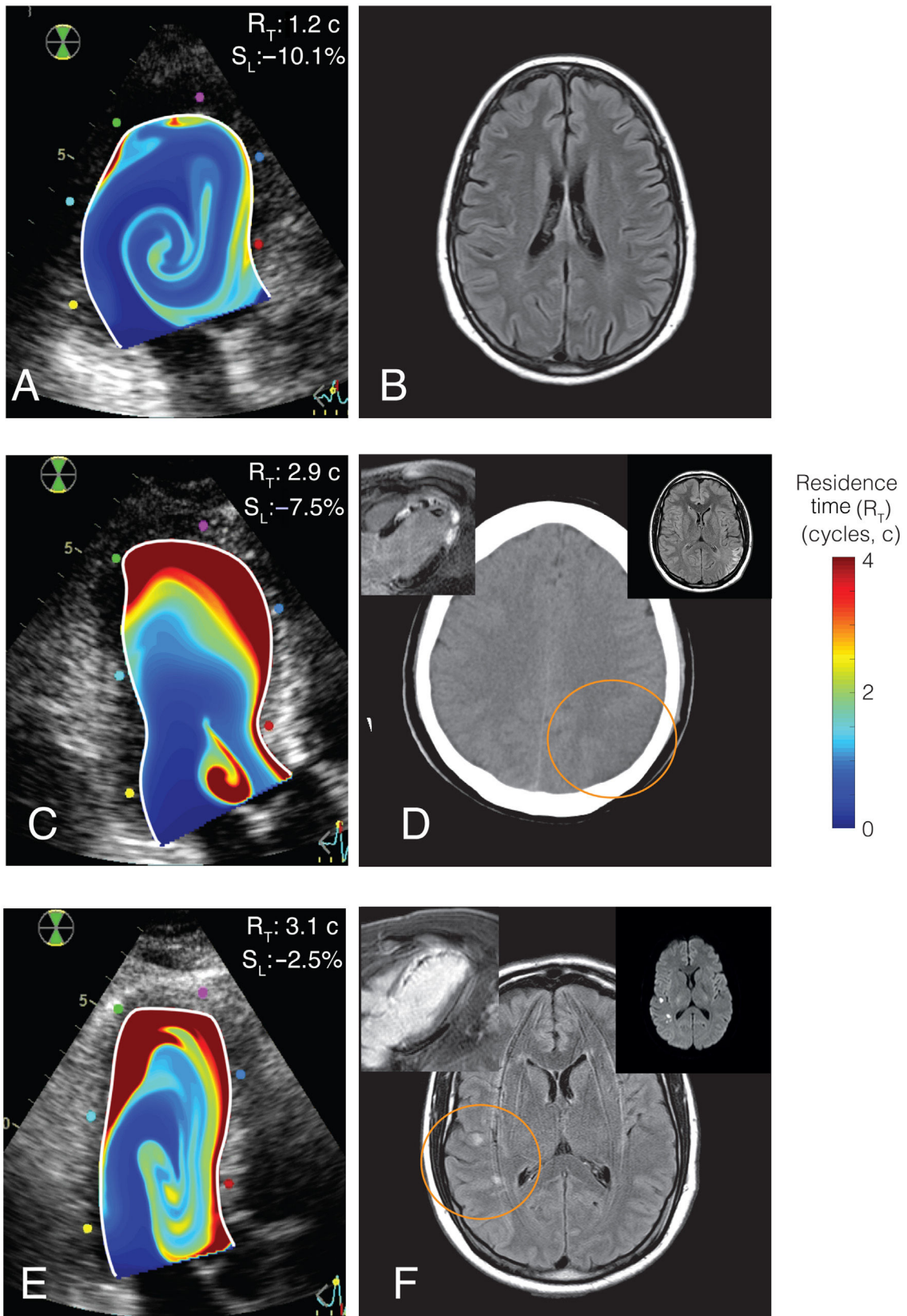


Figure 4. Representative examples of residence time imaging and the primary endpoint. A, B, R_T mapping and T₂-FLAIR brain MR of a patient with no primary endpoint. C, D, R_T mapping and brain computed tomography of a patient with an ischemic stroke and LV mural thrombosis (inserts: CMR and T₂-FLAIR brain MR). E, F, R_T mapping and T₂-FLAIR brain imaging of a patient with a SBI (inserts: CMR and brain diffusion-weighted MRI, showing the acute nature of the lesions). In all cases, R_T mapping is overlaid on the B-mode echocardiogram. Upper-right corner in panels A, C and E, individual values of apical strain, S_L , and residence time, R_T .

Ultrasound for addressing cardioembolic risk after STEMI

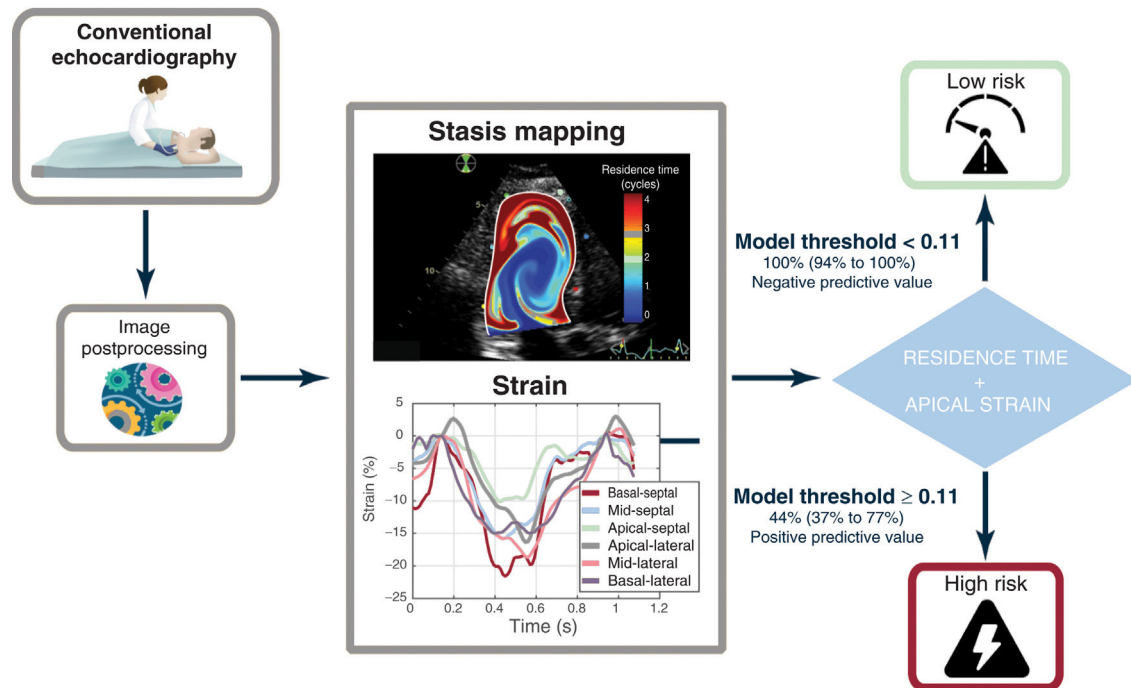


Figure 5. Central illustration. Potential algorithm for addressing the risk of cardioembolism after myocardial infarction based on the results of stasis imaging and strain; STEMI, ST-segment elevation myocardial infarction.

condition leading to cognitive impairment and which doubles the risk of stroke.¹⁴ Brain MR is the gold standard for the diagnosis of SBI, and diffusion-weighted images allow the timing of SBI lesions to be identified within a few hours of their occurrence, therefore discriminating acute, subacute, and chronic injuries. SBIs are a sensitive proxy of cardioembolic risk in several cardiac diseases and procedures, as well as a source of disability and mortality *per se*.¹⁵ The results of our study prospectively demonstrate a temporal association between SBIs and STEMI, which has been indirectly suggested by the frequent finding of myocardial scars in patients with SBIs.¹⁶ Nevertheless, whether both indices remain predictors of cardioembolism in other settings needs to be addressed. We observed a 6-month incidence of SBIs of 6% in our STEMI population, and half of the patients with SBI also showed LVT. In 1 patient, the identification of SBI was followed by an ischemic stroke a few days later. Furthermore, 1 stroke occurred in a patient in whom LVT had been identified and anticoagulation initiated in the setting of this comprehensive research-related imaging workup. This complication highlights the limitations of current stroke prevention guided exclusively by the visualization of mural thrombosis,^{5,17} and illustrates the potential advantage of anticipating anticoagulation before the development of local thrombosis. Although SBIs can be caused by the cardiac catheter interventions *per se*,¹⁸ the observation of concomitant mural thrombosis in 1 patient and a subsequent stroke in another suggests catheter manipulation as a highly unlikely source of SBIs in our cohort.

Blood stasis is a key factor in Virchow's triad that leads to thrombosis.⁶ However, current methods for quantifying stasis in the heart are qualitative and limited. Although spontaneous contrast is related to the risk of thrombosis both in the left atrium¹⁹ and the LV,²⁰ spontaneous contrast is highly dependent

on operator, equipment, and nonfluidic rheological factors.²¹ Technological advances in the last decade open up the opportunity of obtaining time-resolved 2- or even 3-dimensional flow velocity fields from imaging modalities.^{7,22} Applying the physical laws of fluid dynamics to these velocity fields allows quantitative indices to be derived that account for the transport of blood inside the chambers, the interaction between incoming fresh blood and the remnant pool, and the residual stasis. It has been demonstrated that the average R_T of blood in the LV closely correlates with the number of high-intensity signals detected by carotid Doppler ultrasound in a porcine model of STEMI.¹¹ In another pilot clinical study, R_T was also higher in patients who showed mural thrombosis during the subacute phase of STEMI.¹⁰ Blood transport in the LV is a complex phenomenon, governed by fluid-structure and fluid-dynamical interplays which are, in turn, sensitive to early vs late filling fractions, the degree of chamber emptying, and the development of the diastolic vortex ring.^{7,9,23} This explains why the risk of mural thrombosis after STEMI is related to an abnormal apical flow transport.^{24,25} These aspects can only be indirectly inferred by visual inspection of velocity fields but can be very accurately analyzed and quantified using stasis imaging.

The second factor of Virchow's triad is related to the tissue changes in the vessel walls. Endocardial injury and collagen exposure activate the coagulation system locally, and the extent of local damage is closely related to the risk of thrombosis. In the setting of STEMI, the degree of impairment of myocardial longitudinal strain is closely related to the transmural extent of myocardial necrosis.²⁶ In our study, apical strain was related to cardioembolic risk²⁷ but was not mediated by increased intraventricular stasis,²⁸ as apical strain did not correlate with R_T .

Clinical implications

This study suggests a new opportunity for a clinical trial assessing the efficacy of OAC in selected patients guided by stasis imaging. Anticipating a 45% probability of suffering a cardioembolic event based on imaging (the positive predictive value of our model) is a risk-benefit ratio that justifies initiating anticoagulation in this subgroup of patients with STEMI. Once initiated, monitoring stasis imaging could potentially also be useful to discontinue anticoagulation whenever strain and R_T return to near normal values. Idiosyncratic coagulation blood-related factors may potentially account for the finding of only a 45% positive predictive value of the imaging model. Interestingly, these coagulation factors can be efficiently incorporated to the fluid dynamics models to obtain integrated metrics of thrombosis.²⁹ A negative predictive value > 95% suggests that very few patients at risk would be left untreated. These findings should be confirmed by further external validation.

After an embolic stroke of unknown source, the benefit of anticoagulation needs to be balanced against bleeding risk,⁴ and stasis imaging may also be useful in this setting. Remarkably, blood stasis using R_T can also be quantified inside the left atrium and the left atrial appendage.³⁰ Because LV systolic dysfunction, atrial myopathy and disturbed intra-atrial flow are highly prevalent in patients with an embolic stroke of unknown source,³¹ stasis imaging may also be useful in this condition. This technique may also provide insights into the relationship between subclinical LV systolic dysfunction and silent cerebrovascular disease.⁴

Limitations

The number of patients and events was relatively small, with nonnegligible losses during follow-up. Thus, the results of this study should be taken with caution and interpreted as hypothesis-generating. They should also be validated in further studies. Despite the inclusion criteria establishing an EF \leq 45% in the screening exam, EF was > 50% in 20 patients at the time of the enrollment echocardiogram (performed within 72 hours of inclusion) due to early recovery of systolic function after revascularization. The primary endpoint integrated events of different clinical relevance. Although this may lower the prognostic implications of our findings, the composite primary endpoint is supported by: a) the well-established relationship between neurological and imaging outcomes summarized above, and b) the poor prognostic implications of LV mural thrombosis after STEMI.¹⁷ SBIs and neurological events cannot be unequivocally attributed to a cardioembolic origin and alternative etiologies are plausible. To minimize this limitation, we performed a comprehensive etiological workup in all patients with SBIs and implanted cardiac monitoring devices in a random sample of patients. Nevertheless, it is impossible to completely exclude small vessel disease or subclinical AF as causing the identified lesions. The role of catheterization procedures as a source of SBIs *per se* has been discussed above. The 25% incidence of the primary endpoint may seem higher than in other series. However, this could be due to the strict inclusion criteria, focusing on patients with LV systolic dysfunction at admission and undergoing comprehensive serial cardiac and brain imaging assessment. As anticipated, not all patients underwent full follow-up procedures for adjudication of the primary endpoint. However, potential verification bias was excluded by a comprehensive imputation sensitivity analysis.

By design, the endpoint time-window was defined between inclusion and the 6-month follow-up visit. However, as 2 patients showed LVT in the enrollment study, we evaluated stasis performance to predict embolism only after this time point (removing these 2 patients from the analyses). The study was

carried out during the SARS-CoV-2 pandemic, which heavily impacted accrual and follow-up rates. Furthermore, for patients in the study from March 2020 and onwards, procoagulant states related to COVID-19 infection and/or vaccination cannot be completely excluded.

There are some limitations regarding stasis imaging. Although our method is based on 2-dimensional transthoracic echocardiography and assumes a planar-flow distribution, appropriate validation studies show that the error related to this assumption is small, and the method shows good reproducibility.^{9,32} Nevertheless, whether the performance of stasis indices is improved when calculated from 3-dimensional CMR data deserves further investigation.⁸

CONCLUSIONS

In patients with STEMI, cardioembolic risk may be predicted using bedside echocardiography combined with stasis imaging. This imaging modality appears to be well-suited for personalizing primary prevention in patients with impaired systolic function and no history of AF.

WHAT IS KNOWN ABOUT THE TOPIC?

Patients with ST-segment elevation myocardial infarction are at risk of cardioembolic stroke when ejection fraction is reduced. However, in clinical trials under these conditions, bleeding has neutralized the benefit of OAC.

WHAT DOES THIS STUDY ADD?

Digital processing of conventional color-Doppler echocardiograms can be used to obtain 2-dimensional maps of intraventricular blood stasis in the left ventricle. Quantitative metrics of stasis can be used to assess cardioembolic risk, thereby allowing physicians to identify patients at high/low risk and to select or exclude candidates for primary prevention.

FUNDING

This study was supported by the *Instituto de Salud Carlos III* (PI15/02211-ISBITAMI and DTS/1900063 -ISBIFLOW), the *Comunidad de Madrid* (Synergy Grant: Y2018/BIO-4858 PREFI-CM) and by the EU—European Regional Development Fund. JCdA was partially supported by NIH grants R01HL158667 and NIH R01HL160024.

ETHICAL CONSIDERATIONS

The study was approved by the Ethics Committee of *Hospital Gregorio Marañón*, and all patients provided written informed consent. The study was academically funded, and the *Fundación para la Investigación Biomédica Hospital Gregorio Marañón* was the sole sponsor. The work conforms to the principles outlined in the Declaration of Helsinki.

This work adheres to the Sex and Gender Equity in Research (SAGER) guidelines by integrating sex and gender variables in all aspects of our research.

STATEMENT ON THE USE OF ARTIFICIAL INTELLIGENCE

No artificial intelligence methods or tools were used when preparing or drafting the manuscript, or when analyzing the data.

AUTHORS' CONTRIBUTIONS

E. Rodríguez-González, P. Martínez-Legazpi, T. Mombiela, A. González-Mansilla, A. Delgado-Montero, J.A. Guzmán-De-Villoria, F. Díaz-Otero, R. Prieto-Arévalo, M. Juárez, M.C. García del Rey, A. Postigo, R. Yotti, M. García-Villalba, J.C. del Álamo, J. Bermejo made substantial contributions to the conception or design of the work; or the acquisition, analysis, or interpretation of data for the work. E. Rodríguez-González, P. Martínez-Legazpi, P. Fernández-García, Ó. Flores, F. Fernández-Avilés, J.C. del Álamo and J. Bermejo made substantial contributions by drafting the work or revising it critically for important intellectual content; P. Martínez-Legazpi, F. Fernández-Avilés, J.C. del Álamo and J. Bermejo gave the final approval of the version to be published; and P. Martínez-Legazpi, J.C. del Álamo and J. Bermejo agree to be accountable for all aspects of the work.

CONFLICTS OF INTEREST

P. Martínez-Legazpi, J.C. del Álamo, R. Yotti, and J. Bermejo are inventors of a method for quantifying intracardiac stasis and shear stresses from imaging data under a Patent Cooperation Treaty application (WO2017091746A1). The remaining the authors have nothing to disclose.

APPENDIX. SUPPLEMENTARY DATA

Supplementary data associated with this article can be found in the online version available at <https://doi.org/10.1016/j.rec.2024.04.007>.

REFERENCES

- Sundboll J, Horvath-Puho E, Schmidt M, et al. Long-Term Risk of Stroke in Myocardial Infarction Survivors: Thirty-Year Population-Based Cohort Study. *Stroke*. 2016;47:1727–1733.
- Alexander JH, Lopes RD, James S, et al. Apixaban with antiplatelet therapy after acute coronary syndrome. *N Engl J Med*. 2011;365:699–708.
- Mega JL, Braunwald E, Wiviott SD, et al. Rivaroxaban in patients with a recent acute coronary syndrome. *N Engl J Med*. 2012;366:9–19.
- Ntaios G, Vemmos K, Lip GY. Oral anticoagulation versus antiplatelet or placebo for stroke prevention in patients with heart failure and sinus rhythm: Systematic review and meta-analysis of randomized controlled trials. *Int J Stroke*. 2019;14:856–861.
- Camaj A, Fuster V, Giustino G, et al. Left ventricular thrombus following acute myocardial infarction: JACC state-of-the-art review. *J Am Coll Cardiol*. 2022;79:1010–1022.
- Watson T, Shantsila E, Lip GY. Mechanisms of thrombogenesis in atrial fibrillation: Virchow's triad revisited. *Lancet*. 2009;373:155–166.
- Bermejo J, Martínez-Legazpi P. *Ann Rev Fluid Mech*. 2015;47:315–342.
- Rossini L, Martínez-Legazpi P, Vu V, et al. A clinical method for mapping and quantifying blood stasis in the left ventricle. *J Biomech*. 2016;49:2152–2161.
- Benito Y, Martínez-Legazpi P, Rossini L, et al. Age-Dependence of Flow Homeostasis in the Left Ventricle. *Front Physiol*. 2019;10:485.
- Martínez-Legazpi P, Rossini L, Pérez Del Villar C, et al. Stasis Mapping Using Ultrasound: A Prospective Study in Acute Myocardial Infarction. *JACC Cardiovasc Imaging*. 2018;11:514–515.
- Delgado-Montero A, Martínez-Legazpi P, Desco MM, et al. Blood Stasis Imaging Predicts Cerebral Microembolism during Acute Myocardial Infarction. *J Am Soc Echocardiogr*. 2020;33:389–398.
- García D, Del Álamo JC, Tanne D, et al. Two-dimensional intraventricular flow mapping by digital processing conventional color-Doppler echocardiography images. *IEEE Trans Med Imaging*. 2010;29:1701–1713.
- Russo C, Jin Z, Homma S, et al. Subclinical left ventricular dysfunction and silent cerebrovascular disease: the Cardiovascular Abnormalities and Brain Lesions (CABL) study. *Circulation*. 2013;128:1105–1111.
- Gupta A, Giambrode AE, Gialdini G, et al. Silent brain infarction and risk of future stroke: A systematic review and meta-analysis. *Stroke*. 2016;47:719–725.
- Fanning JP, Wesley AJ, Wong AA, et al. Emerging spectra of silent brain infarction. *Stroke*. 2014;45:3461–3471.
- Takasugi J, Yamagami H, Noguchi T, et al. Detection of left ventricular thrombus by cardiac magnetic resonance in embolic stroke of undetermined source. *Stroke*. 2017;48:2434–2440.
- Lattuca B, Bouziri N, Kerneis M, et al. Antithrombotic therapy for patients with left ventricular mural thrombus. *J Am Coll Cardiol*. 2020;75:1676–1685.
- Hassell ME, Nijveldt R, Roos YB, et al. Silent cerebral infarcts associated with cardiac disease and procedures. *Nat Rev Cardiol*. 2013;10:696–706.
- Daniel WG, Nellesen U, Schröder E, et al. Left atrial spontaneous echo contrast in mitral valve disease: an indicator for an increased thromboembolic risk. *J Am Coll Cardiol*. 1988;11:1204–1211.
- Kozdag G, Ciftci E, Vural A, et al. Silent cerebral infarction in patients with dilated cardiomyopathy: echocardiographic correlates. *Int J Cardiol*. 2006;107:376–381.
- Merino A, Hauptman P, Badimon L, et al. Echocardiographic “smoke” is produced by an interaction of erythrocytes and plasma proteins modulated by shear forces. *J Am Coll Cardiol*. 1992;20:1661–1668.
- Hong GR, Pedrizzetti G, Tonti G, et al. Characterization and quantification of vortex flow in the human left ventricle by contrast echocardiography using vector particle image velocimetry. *JACC Cardiovasc Imaging*. 2008;1:705–717.
- Bolger AF, Heiberg E, Karlsson M, et al. Transit of blood flow through the human left ventricle mapped by cardiovascular magnetic resonance. *J Cardiovasc Magn Reson*. 2007;9:741–747.
- Garg P, van der Geest RJ, Swoboda PP, et al. Left ventricular thrombus formation in myocardial infarction is associated with altered left ventricular blood flow energetics. *Eur Heart J Cardiovasc Imaging*. 2019;20:108–117.
- Van Dantzig JM, Delemarre BJ, Bot H, et al. Doppler left ventricular flow pattern versus conventional predictors of left ventricular thrombus after acute myocardial infarction. *J Am Coll Cardiol*. 1995;25:1341–1346.
- Cimino S, Canali E, Petronilli V, et al. Global and regional longitudinal strain assessed by two-dimensional speckle tracking echocardiography identifies early myocardial dysfunction and transmural extent of myocardial scar in patients with acute ST elevation myocardial infarction and relatively preserved LV function. *Eur Heart J Cardiovasc Imaging*. 2013;14:805–811.
- Olsen FJ, Pedersen S, Galatius S, et al. Association between regional longitudinal strain and left ventricular thrombus formation following acute myocardial infarction. *Int J Cardiovasc Imaging*. 2020;36:1271–1281.
- Neskovic AN, Marinkovic J, Bojic M, et al. Predictors of left ventricular thrombus formation and disappearance after anterior wall myocardial infarction. *Eur Heart J*. 1998;19:908–916.
- Guerrero-Hurtado M, García-Villalba M, Gonzalo A, et al. Efficient multi-fidelity computation of blood coagulation under flow. *PLoS Comput Biol*. 2023;19:e1011583.
- García-Villalba M, Rossini L, Gonzalo A, et al. Demonstration of Patient-Specific Simulations to Assess Left Atrial Appendage Thrombogenesis Risk. *Front Physiol*. 2021;12:596596.
- Spartera M, Stracquadanio A, Pessoa-Amorim G, et al. The impact of atrial fibrillation and stroke risk factors on left atrial blood flow characteristics. *Eur Heart J Cardiovasc Imaging*. 2021;23:115–123.
- Bermejo J, Benito Y, Alhama M, et al. Intraventricular vortex properties in non-ischemic dilated cardiomyopathy. *Am J Physiol Heart Circ Physiol*. 2014;306:H718–H729.